Paper No.
08333

NACE INTERNATIONAL CORROSION 2008 CONFERENCE & EXPO

THE EFFECT OF ACETIC ACID ON THE INTEGRITY OF PROTECTIVE IRON CARBONATE LAYERS IN CO_2 CORROSION OF MILD STEEL

Vanessa Fajardo, Christian Canto, Bruce Brown, David Young and Srdjan Nesic
Ohio University
Institute for Corrosion and Multiphase Technology
Dept. of Chemical Engineering
342 West State Street
Athens, OH 45701

ABSTRACT

The role of acetic acid on the integrity of the protective iron carbonate layer ($FeCO_3$) formed on X-65 mild steel in carbon dioxide corrosion has been investigated. Three sets of experiments were conducted, by varying the acetic acid concentration, flow velocity and pH. It was found that the presence of acetic acid may lead to the damage of the iron carbonate layer and a temporary increase in the corrosion rate. However, the final corrosion rate did not seem to be affected as much.

Keywords: acetic acid, CO_2 corrosion, iron carbonate layer, buffered acetic acid solution, X65 mild steel

INTRODUCTION

Acetic acid is the most prevalent of the different organic acids detected in oilfield brines and has been found to contribute to a drastic increase in internal pipeline corrosion.[1] As a rule of thumb, when the concentration of acetic acid is found to be higher than 1mM, the typical CO_2 corrosion rate can increase significantly, and the localized attack mode is more prevalent [2].

The formation of iron carbonate ($FeCO_3$) as the main corrosion product in CO_2 corrosion is possible when the concentrations of Fe^{2+} and CO^{3-} exceed the solubility product. Iron carbonate precipitation is highly dependent on the supersaturation and temperature[3,4]. The formation of an iron carbonate layer on the steel surface is known to retard the corrosion rate. This corrosion product layer can act as barrier that limits the transport of species from the bulk to the steel surface or vice-versa[4]. Previous research has identified that the presence of acetic acid does not affect the $FeCO_3$ layer protectiveness. However, it was observed that the presence of organic acid does prolong the formation of a protective layer [5].

This paper evaluates the effect of acetic acid on the integrity and protectiveness of the iron carbonate layer on mild steel. A slightly different procedure was used compared to the previous studies [5-7] and

three key parameters were examined: concentration of undissociated acetic acid, flow velocity, and pH. In the present work, the acetic acid was always added as a buffered aqueous solution to allow independent control of the pH.

EXPERIMENTAL PROCEDURE

A three-electrode setup was used in all the experiments and is shown in Figure 1. X65 mild steel material was used for the rotating cylinder electrode (RCE), which served as the working electrode (WE). A platinum wire was used as a counter electrode (CE) with a saturated silver-silver chloride (Ag/AgCl) reference electrode (RE). The pH was continuously monitored throughout each experiment with an electrode immersed in the electrolyte. The temperature was regulated using a thermocouple immersed in the solution and a controller linked to a hot plate.

The glass cell was filled with 2 liters of electrolyte, which was made from de-ionized water and 3 mass% NaCl. In all experiments, CO_2 was continuously bubbled through the electrolyte for approximately 1 hour before the experiment and during the entire experiment. This was done in order to ensure that all the dissolved oxygen was removed and to maintain saturation with CO_2 of the test solution. When needed, a hydrochloric acid (HCl) or sodium bicarbonate ($NaHCO_3$) solution was added to adjust the pH. The experimental temperature was maintained at 80 ±1°C in all experiments.

To begin each experiment, the steel WE surface was polished using 240, 320, 400 and 600 grit silicon carbide (SiC) paper wetted with isopropanol, dried, mounted on the specimen holder, and immersed into the electrolyte. The free corrosion potential was immediately measured. Polarization resistance (R_p) measurements were conducted by polarizing the WE ±5mV from the E_{oc} (free corrosion potential) at a scan rate of 0.1mV/s. The solution resistance (R_s) was measured independently using alternating current (AC) impedance and the measured R_p was then corrected. AC impedance measurements were done by applying an sinusoidal potential (±5mV peak-to-peak amplitude) around the E_{oc} to the WE using the frequency range of 1Hz to 100kHz.

Three sets of experiments were conducted, using the experimental conditions defined in Table 1, to evaluate the effect of acetic acid on the integrity of the iron carbonate layer. Effect of the flow velocity and pH in the presence of acetic acid were also evaluated.

The first set of experiments was designed to see the influence of acetic acid on the iron carbonate layer at a constant pH. Therefore, the acetic acid was added into the system as a buffered acetic acid solution. The conjugate acid-base pair was acetic acid, CH_3COOH, and acetate ion, CH_3COO^- supplied as a soluble salt, such as sodium acetate trihydrate $NaC_2H_3O_2 \cdot 3H_2O$. The physical and chemical properties of acetic acid are shown in Table 2. Experiments were carried out with two different undissociated acetic acid concentrations, 50 ppm and 100 ppm at pH 6.3 (see Table 3). The total concentration of the acid added into the system was either 1418 ppm or 2836 ppm which was needed to achieve 50 ppm and 100 ppm respectively at pH 6.3. The buffered acetic acid solution was added into the electrolyte only after a protective iron carbonate layer formed as indicated by a reduction in the corrosion rate to or below 0.1 mm/y. All tests in this series were conducted at 80°C, 1 bar total pressure (0.56 bar pCO_2, balance pH_2O), 3 mass % NaCl, pH 6.3 and stagnant conditions. The initial $FeCO_3$ supersaturation was set to 100. Therefore the supersaturation rapidly decreased as iron carbonate precipitated and the solution drifted back toward thermodynamic equilibrium.

The effect that the flow velocity has on the integrity and protectiveness of the iron carbonate layer in presence of acetic acid was evaluated in the second set of experiments. The iron carbonate layer was developed under different rotational velocities (stagnant conditions, 100, and 1000 rpm). The rotational velocity was maintained constant during each velocity test. These experiments were also conducted at 80°C, 0.56 bar pCO_2, 3mass% NaCl, 50 ppm undissociated HAc, and pH 6.3. The initial supersaturation was 100.

Finally, the third set of experiments was conducted to see the effect of pH decrease during acetic acid addition. Once the iron carbonate layer formed at 80°C, 0.56 bar pCO_2, 3mass% NaCl, pH 6.3 and initial supersaturation 100, the buffered acetic acid solution (with 50 ppm of free HAc) was added into the system. The pH of the buffered solution was allowed to drop to pH 6.0. This was achieved since the buffered solution that was added was made with a smaller amount of acetate salt. (Table 4).

Analysis of the corrosion product layer was performed using scanning electron microscope (SEM), energy dispersive x-ray analysis (EDX) and x-ray diffraction (XRD).

RESULTS AND DISCUSSION

A large number of baseline experiments with only then iron carbonate layer formation in pure CO_2 corrosion (in the absence of acetic acid) have been conducted at pH 6.3. At the beginning of each experiment, the corrosion rate on the bare steel surface was typically 1 mm/y and decreased within a few days to values which were approximately one order of magnitude lower (< 0.1 mm/y) as iron carbonate layer formed. For the five experiments reviewed here, the acetic acid was added only after the $FeCO_3$ layer formed and the corrosion rate remained stable for 2 days, (in Figure 2, Figure 4, Figure 9, Figure 11 and Figure 13 this is shown by a vertical dotted line).

Influence of acetic acid concentration

In Figure 2, it is seen that the corrosion rate decreased to a low level (≈0.2 mm/y) following formation of an iron carbonate layer. The addition of 50 ppm (0.8 mM) of undissociated acetic acid caused a temporary increase in the corrosion rate to about 0.3 – 0.4 mm/y, However this was followed by a another decrease and within a day the corrosion rate settled back to ≈0.2 mm/y and remained constant beyond that point. In Figure 4, it is shown that in another similar experiment, the addition of 100 ppm (1.6 mM) of undissociated acetic acid increased the corrosion rate up to 1.4 mm/y. However, this effect was also temporary. After a few days the corrosion rate was returned to the low values below 0.2 mm/y. This behaviour correlated with the previous work.[5, 6] Since the corrosion rate only temporarily increased with addition of acetic acid and eventually returned to the low values it had before the acetic acid was added, it was assumed that the protective iron carbonate layer was not affected by the acid, as reported earlier. [5, 6]

However, SEM images show a significant loss of iron carbonate crystals from the surface morphology following the addition of acetic acid, and even greater loss when the concentration of undissociated acetic acid was doubled from 50 to 100 ppm (Figure 3b and Figure 5b). This seems to support the view expressed by Gulbrandsen et al.[7] that the solubility of the iron carbonate increases in the presence of the acid even if the pH is maintained (presumably via complex formation). However, a more careful examination of the SEM images shows that the surviving crystals still have sharp edges and maintain the rhombohedral shape which is not a signature of the crystal dissolution process. Dissolution typically leads to rounding of the crystal edges and a diffuse “popcorn-like” appearance of the dissolving iron

carbonate layer. Therefore, it is suspected that the acid did not affect the solubility of the iron carbonate directly, but rather has diffused through the pores of the layer and directly attacked the steel underneath (as evidenced by the temporary increase in the corrosion rate seen in Figure 2 and Figure 4). This has lead to the undermining of the iron carbonate layer and the weakening of bond between the iron carbonate and the steel, which eventually lead to loss of parts of the layer by detachment. It was difficult to directly detect or capture these detached iron carbonate particles as the test cell already contained a significant amount of loose iron carbonate crystalline material which precipitated in the first few days of the experiment. The surviving iron carbonate crystals which remained attached to the steel surface after the addition of the acid were on average larger when compared to the ones detected before the addition of the acid, which can be easily explained by the fact that the solution remained supersaturated after the addition of the acid and the precipitation process continued.

In conjunction with the SEM, the energy dispersive X-ray analysis (EDX) was used to confirm the elements present in the layer seen on the X65 mild steel. Figure 7 shows EDX analysis of (a) a crystal seen on the steel surface following the attack by acetic acid, and (b) an exposed substrate, i.e. the space where the crystal was removed. Although EDX is a semi-quantitative method, the EDX analysis of the crystals show the peaks, for Fe, O, and C in a approximately 1:1:3 ratio. While the exposed surface only shows the peak of Fe. While this seems logical, a perplexing question remains unanswered: *how can the iron carbonate surface layer which survived the acetic acid attack, which is as porous as the one seen in Figure 3b and Figure 5b still protect the steel surface from corrosion?* Actually this porous layer appears to be as protective as the much denser layer seen before the acid was added (Figure 3a and Figure 5a)

X-ray diffraction (XRD) was used in order to evaluate if there are any other compounds other than $FeCO_3$ which could be identified on the steel surface. The XRD signal shows only weak iron peaks on the sample which has no acetic acid (Figure 8a). This does not happen often, as the 110 reflection of a-Fe is strong, suggesting that the iron carbonate layer deposited over the iron surface is rather thick. On the sample where the addition of 100ppm of undissociated acetic acid caused the steel surface to partially lose some of its iron carbonate crystals, the increase of the main iron peak can be seen (compare Figure 8a to Figure 8b). The experimental data show that the main phase ($FeCO_3$) has an optimal structure, large crystals that provide spots on the 2D-pattern.

Crystalline, semi-crystalline, and amorphous phases are all possibilities in the corrosion product layer. The current XRD analyses could only properly identify crystalline substances such as $FeCO_3$, while the semi-crystalline Fe-compounds such as Fe-salts/hydroxides being much harder to pinpoint. The amorphous phase is not detectable with XRD. In summary, the SEM, EDX and XRD analysis used here were not adequate techniques to help answer the question posed above and more analytical work is ongoing which aims to help elucidate the answer.

Effect of the flow velocity

The effect that flow may exhibit on the integrity of the iron carbonate layer can manifest itself in different ways [4]. The most obvious pathways are the mechanical effects such as shear stress that can lead to or assist removal the iron carbonate crystals. Another possibility is an increase in the transport of dissolved species between the bulk flow and the steel surface. In the experiments without acetic acid, an increase in the sheer stress was observed to cause a decrease in the density of the iron carbonate layer (see Figure 10a. and Figure 12a). This is supported by the corrosion rate measurements shown in Figure 9 and Figure 11. At an increased rotation speed, the corrosion rate is three times higher than in stagnant conditions. The combined effect of the flow and acetic acid addition increased the final corrosion rate to

0.25mm/y at 100 rpm, and to 0.35mm/y at 1000 rpm. Mechanical removal is suspected since the iron carbonate crystals were removed from over 80% of the entire surface at the high shear stress (Figure 12), with no indication of chemical dissolution of the iron carbonate crystals.

Effect of the pH

In order to create somewhat more aggressive conditions in this series of experiments, pH was allowed to decrease from pH 6.3 to pH 6.0 during the addition of acetic acid. It was hypothesized that this might help remove the iron carbonate layer and lead to a sharper increase in the corrosion rate. The analysis of the steel surface from this experiments reveals that the surviving iron carbonate layer had even fewer crystals when compared to the equivalent experiment conducted at a slightly higher pH 6.3 (compare Figure 3b and Figure 14b). However, this did not seem to have any effect on final corrosion rate (see Figure 13 and compare to Figure 2).

CONCLUSIONS

It was found that the presence of acetic acid may lead to damage of the protective iron carbonate layer formed on mild steel. This leads to a temporary increase in the corrosion rate. However, the final corrosion rate does not seem to be affected. It remains unclear how the very porous iron carbonate films surviving the attack by acetic acid continued to protect the underlying steel.

REFERENCES

1. Crolet J.L. and Bonis M.R., "The role of Acetate Ions in CO_2 Corrosion," CORROSION /83, paper no. 160 (Houston, TX: NACE, 1983).
2. M.R. Bonis, J-L. Crolet, "Basics of the Prediction of the Risk of CO_2 Corrosion in Oil and Gas Wells," CORROSION /89, paper no. 466 (Houston TX: NACE 1989).
3. A. Dugstad, "The importance of $FeCO_3$ Supersaturation on the CO_2 Corrosion of mild steel," CORROSION /92, paper no. 14 (Houston TX: NACE 1992).
4. Nesic S., Nordsveen M., Nyborg R., and Stangeland A. "A Mechanistic Model for Carbon Dioxide Corrosion of Mild Steel in the Presence of Protective Iron Carbonate Layers-Part 2: A Numerical Experiment", Corrosion, Volume 59, No.6, 2003, p 489-497.
5. Fajardo V., Canto C., Brown B., and Srdjan N. "Effect of Organic Acids in CO_2 Corrosion", CORROSION /07, paper no. 319 (Houston TX: NACE 2007).
6. O. A. Nafday, S. Nesic, "Iron Layer Formation and CO_2 Corrosion in the Presence of Acetic Acid", CORROSION /05, paper no. 295 (Houston TX: NACE 2005).
7. Gulbrandsen E. "Acetic Acid and Carbon Dioxide Corrosion of Mild steel Covered with Iron Carbonate" CORROSION /07, paper no. 322 (Houston TX: NACE 2007).
8. R.H. Perry, D. Green, Perry's Chemical Engineers' Handbook, 50th ed, McGraw Hill p.2-28 to 2-52.
9. J.A. Dean, "Lange's Handbook of Chemistry," 15th. Edition, McGraw Hill (1999): p.1.15, 8.48

Table 1

Experimental conditions under layer forming

Test solution	Water + 3 mass %NaCl
Test material	API X65
Temperature	80°C
CO_2 Partial Pressure	0.56 bar CO_2
Undissociated (free) organic acid	50 and 100ppm
pH	6.0 and 6.3
Rotation velocity	static, 100 and 1000rpm
Initial supersaturation	100
Sweep rate	0.1 mV/s to 0.2 mV/s
Polarization resistance	From -5mV to 5mV (vs E_{oc})
AC Impedance	± 5mV vs. E_{oc} from 1mHz to 100KHz

Table 2

Physical and chemical properties of acetic acid [8, 9]

	Acetic acid
Formula	CH_3-COOH
Molecular weight	60.05
Density, g/ml at 20°C	1.049
Melting point, °C	16.5
Boiling point, °C	118.1
Acidity (pK_a)	4.76

Table 3

Acetic acid concentration at pH 6.3 and 80°C

Total Concentration	Undissociated acetic acid (ppm)	Acetate concentration (ppm)
1418	50	1368
2836	100	2736

Table 4

Acetic acid concentration at different value of pH at 80°C

pH	Undissociated acetic acid (ppm)	Acetate concentration (ppm)
6.0	50	685
6.3	50	1368

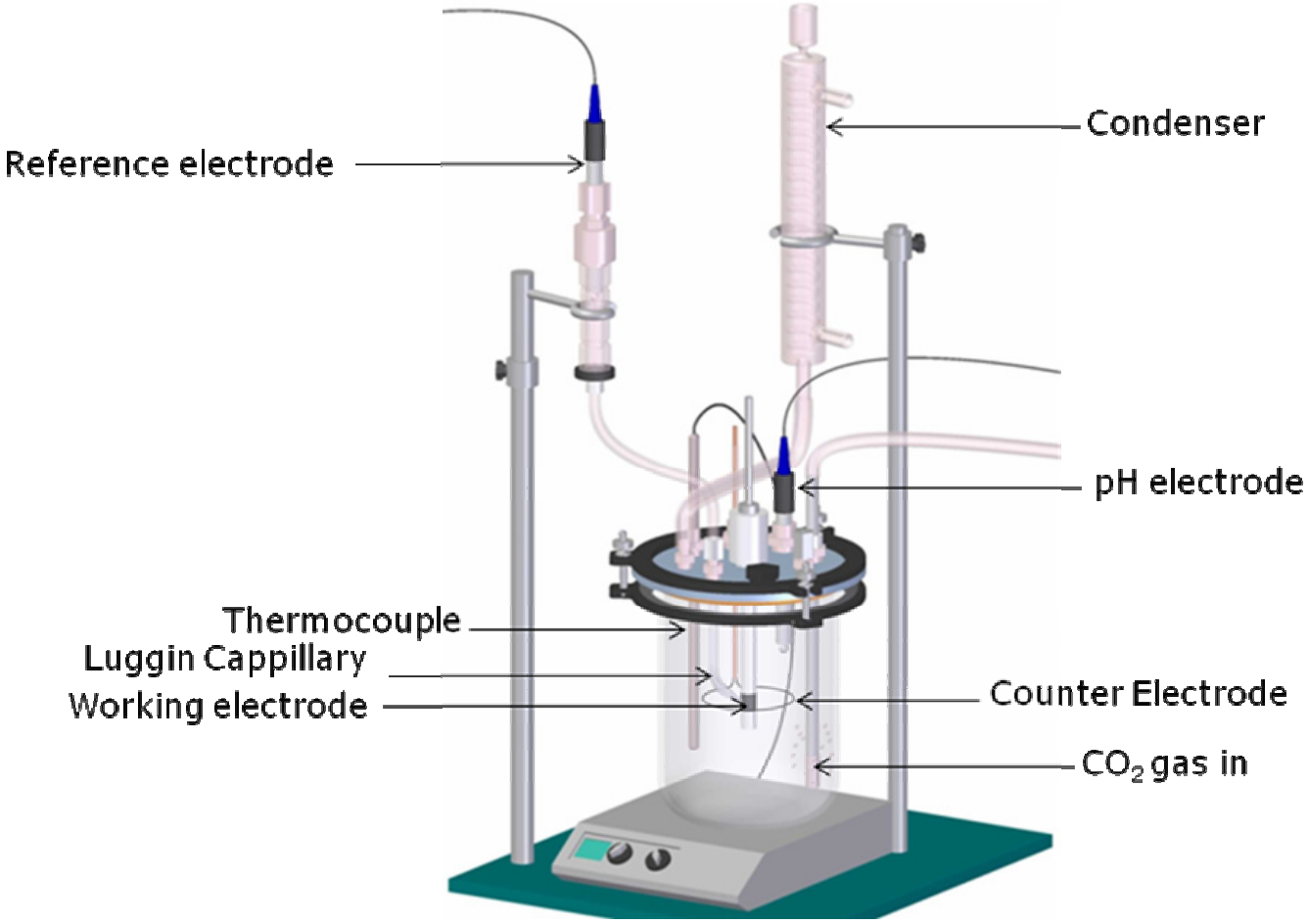

Figure 1. Experimental cell design

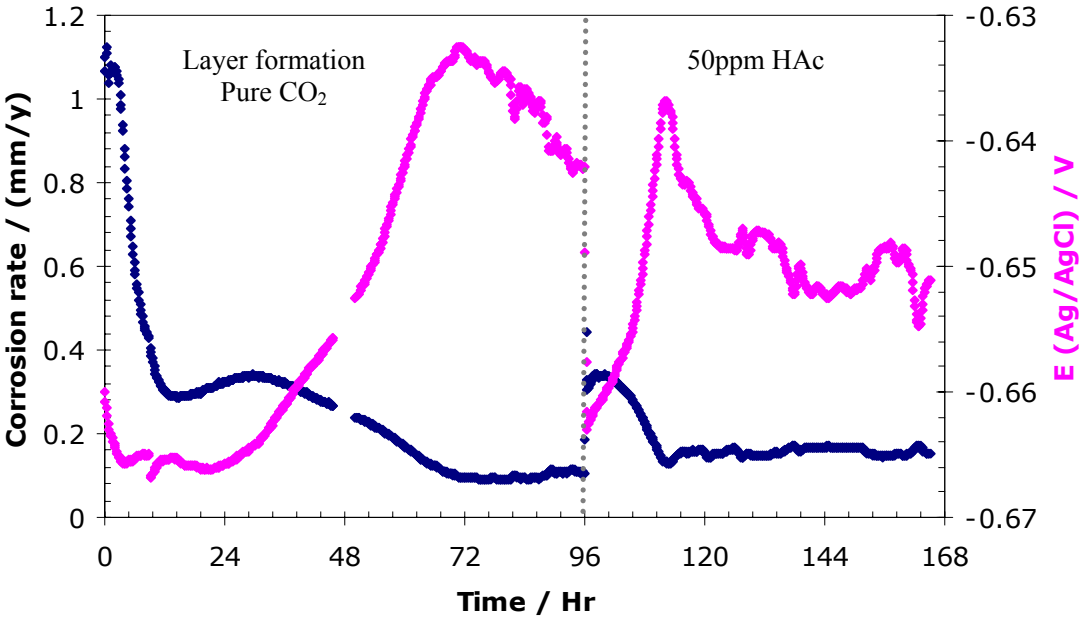

Figure 2. The effect of 50 ppm (0.8 mM) of undissociated acetic acid on the corrosion rate and corrosion potential of X-65 steel during 168 hours of exposure (3% NaCl, pH 6.3, 0.56 bar pCO_2, stagnant conditions and T=80°C).

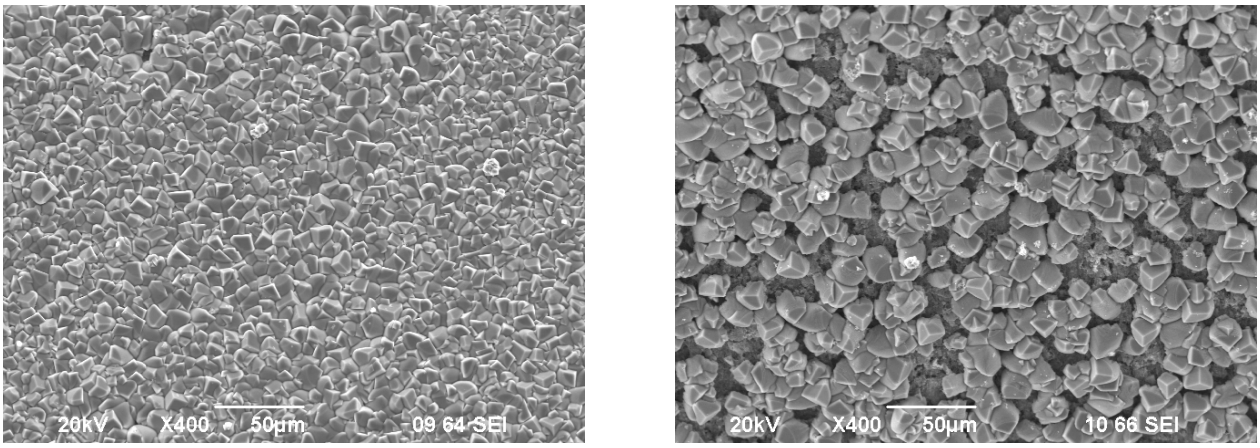

a) b)

Figure 3. $FeCO_3$ layer morphology of X-65 (pCO_2 =0.56 bar, pH 6.3, stagnant conditions and T=80°C).
a) layer formed in pure CO_2 after 96 h, see Figure 2 above and
b) layer after addition of 50 ppm of undissociated acetic acid, appearance at the end of the experiment shown in Figure 2 above.

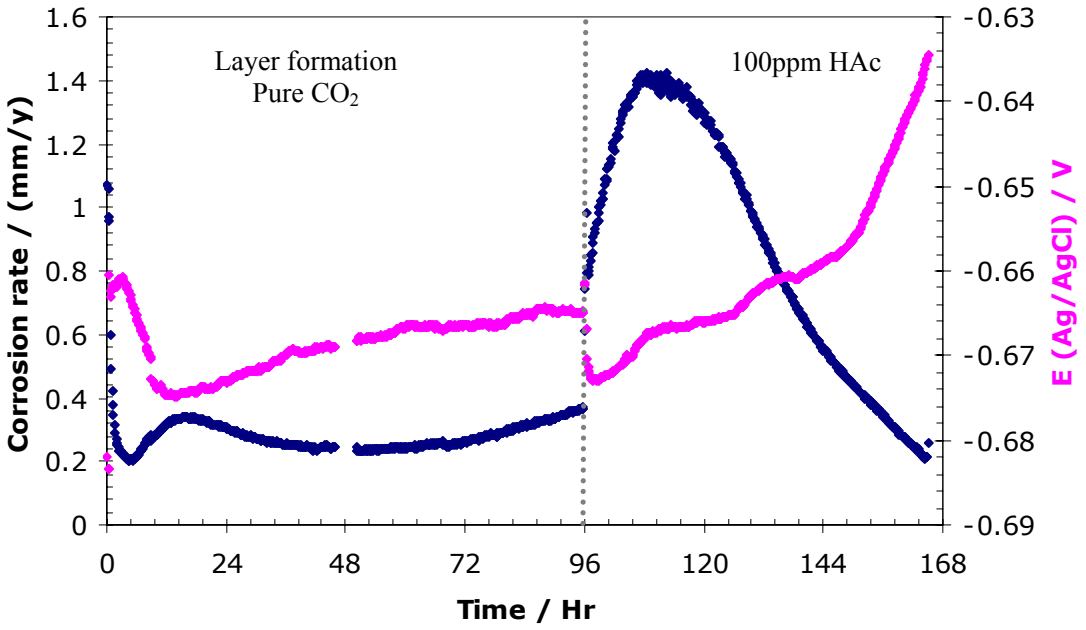

Figure 4. The effect of 100 ppm (1.6 mM) of undissociated acetic acid on the corrosion rate and corrosion potential of X-65 steel during 168 hours of exposure (3% NaCl, pH 6.3, 0.56 bar pCO_2, stagnant conditions and T=80°C).

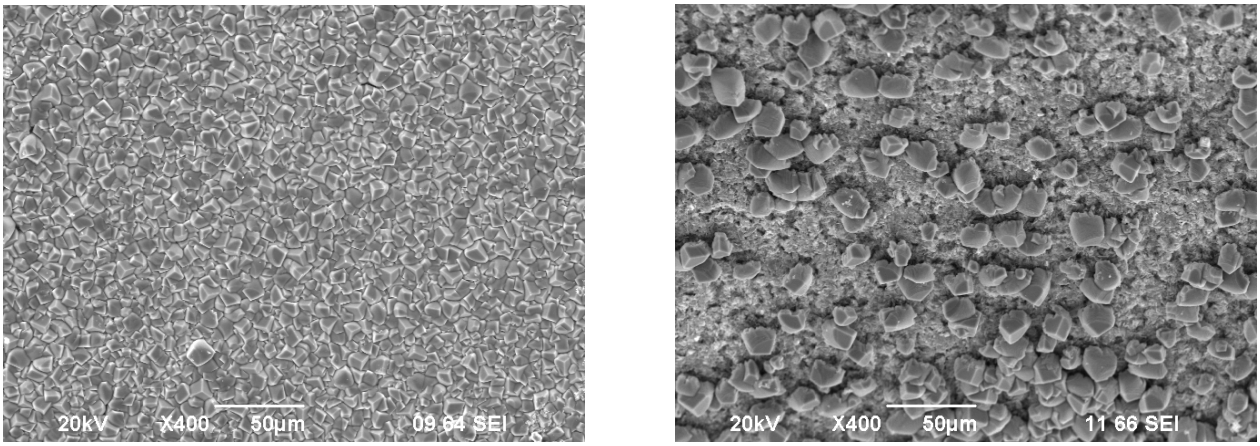

a) b)

Figure 5. $FeCO_3$ layer morphology of X-65 (pCO_2 =0.56 bar, pH 6.3, stagnant conditions and T=80°C).
a) layer formed in pure CO_2 after 96 h, see Figure 4 above and
b) layer after addition of 100 ppm of undissociated acetic acid, appearance at the end of the experiment shown in Figure 4 above.

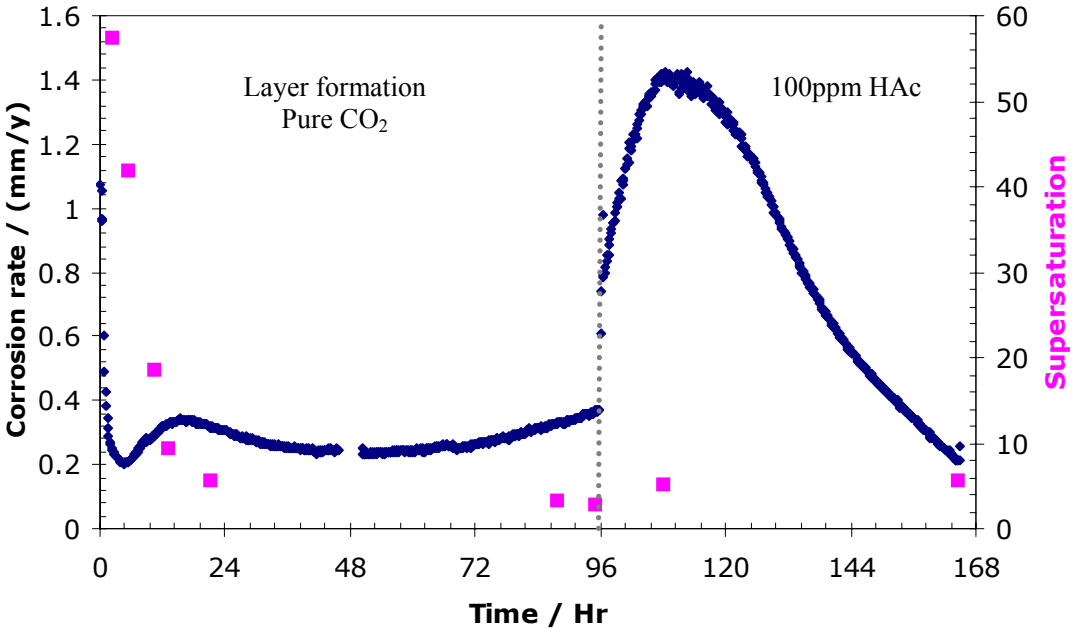

Figure 6. The effect of 100 ppm (1.6 mM) of undissociated acetic acid on the corrosion rate and supersaturation during 168 hours of exposure (3% NaCl, pH 6.3, 0.56 bar pCO_2, stagnant conditions and T=80°C).

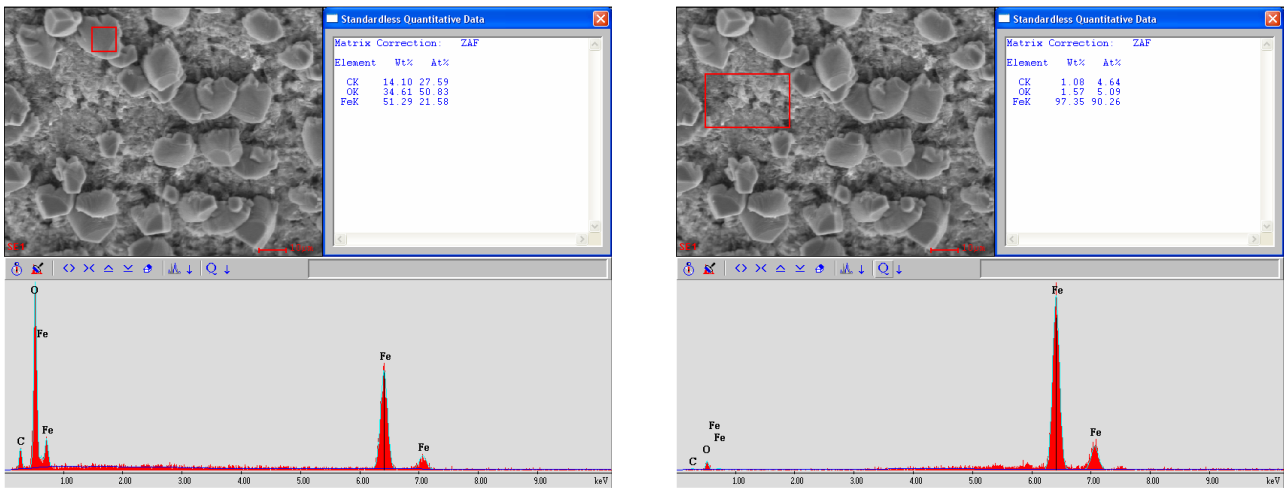

a) b)

Figure 7. EDX analysis of the a) crystal and b) the exposed substrate after the addition of 100 ppm of undissociated acetic acid at pH 6.3, stagnant conditions and T=80°C. Sample taken at the end of the experiment shown in Figure 4 above.

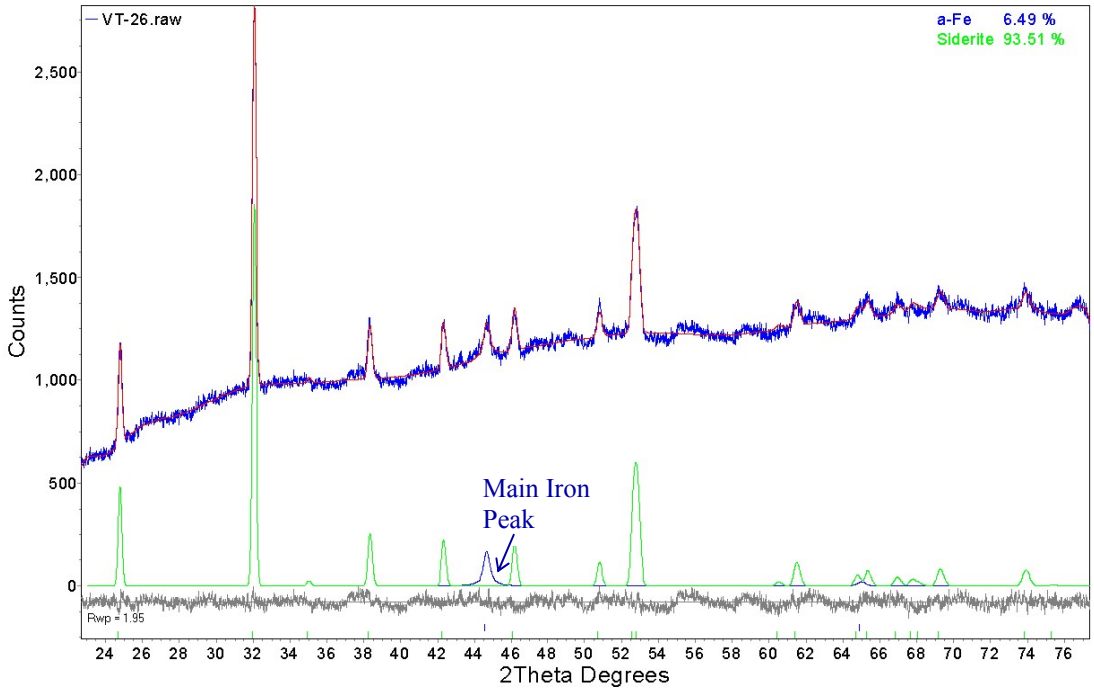

a)

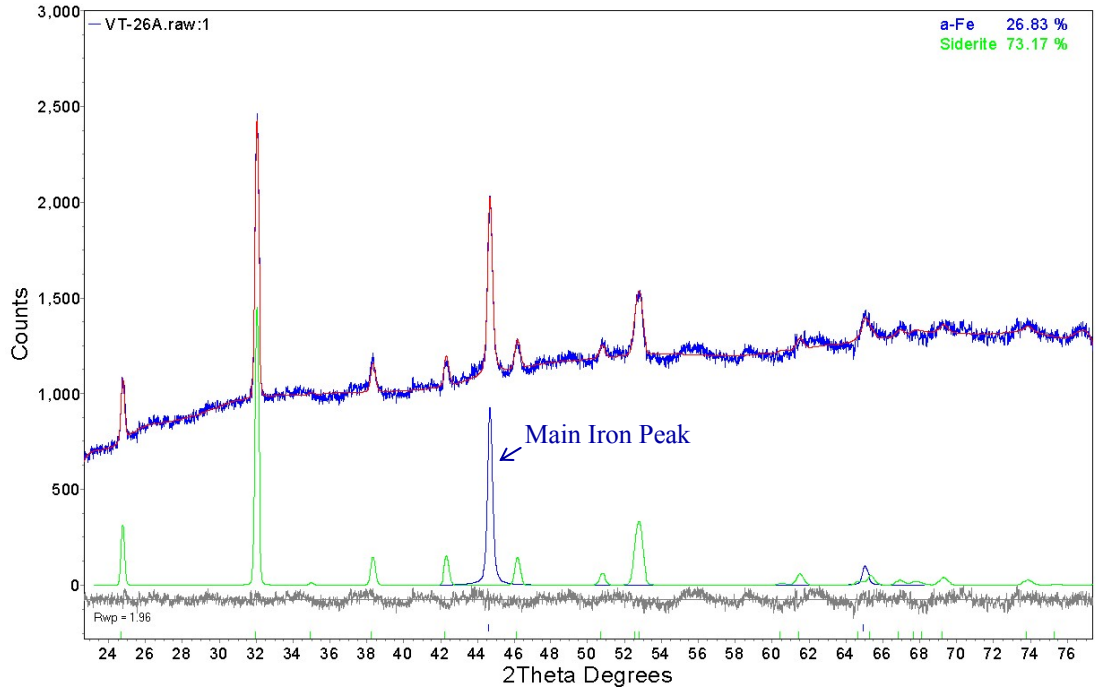

b)

Figure 8. XRD analysis of the layer formed on the steel at pH 6.3, stagnant conditions and T=80°C;
a) layer formed in pure CO_2 after 96 h (without HAc), see Figure 4 above and
b) layer after addition of 100 ppm of undissociated acetic acid, at the end of the experiment shown in Figure 4 above.

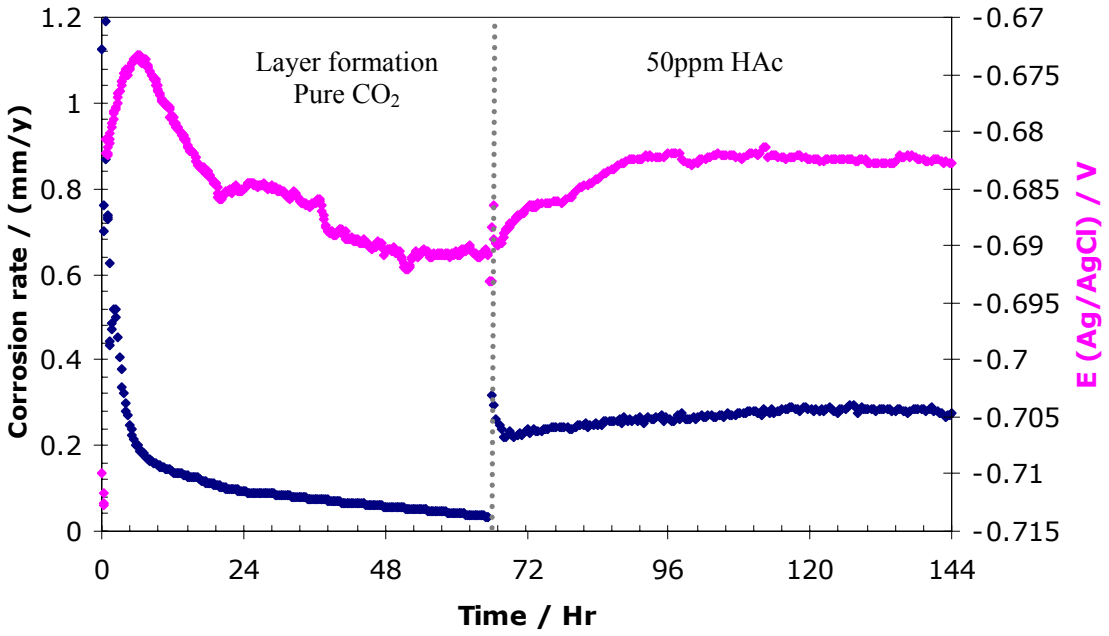

Figure 9. The effect of flow rate on the corrosion rate and corrosion potential of X-65 steel during 168 hours of exposure (3% NaCl, 100 rpm, 50 ppm of undissociated acetic acid, pH 6.3, and T=80°C).

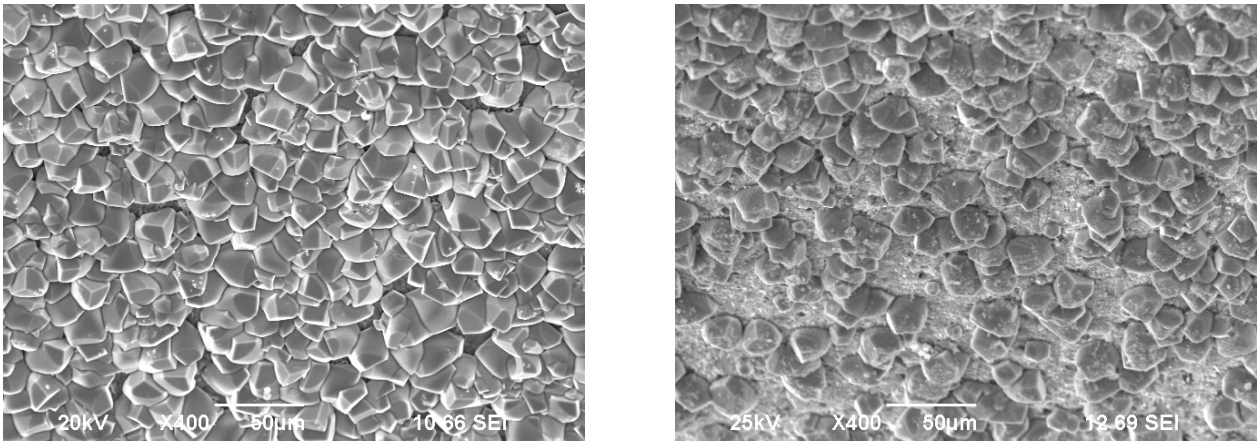

a) b)

Figure 10. $FeCO_3$ layer morphology of X-65 (pCO_2 =0.56 bar, pH 6.3, 100 rpm and T=80°C).
a) layer formed in pure CO_2 after 67 h, see Figure 9 above and
b) layer after addition of 50 ppm of undissociated acetic acid, appearance at the end of the experiment shown in Figure 9 above.

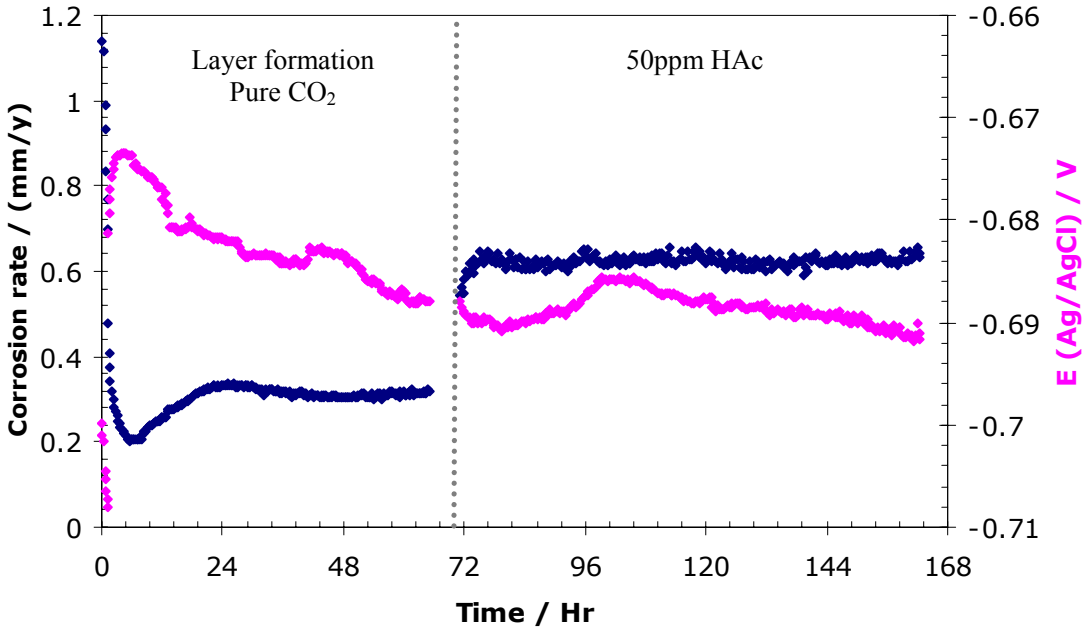

Figure 11. The effect of flow rate on the corrosion rate and corrosion potential of X-65 steel during 168 hours of exposure (3% NaCl, 1000 rpm, 50 ppm of undissociated acetic acid, pH 6.3, 0.56 bar pCO_2, and T=80°C).

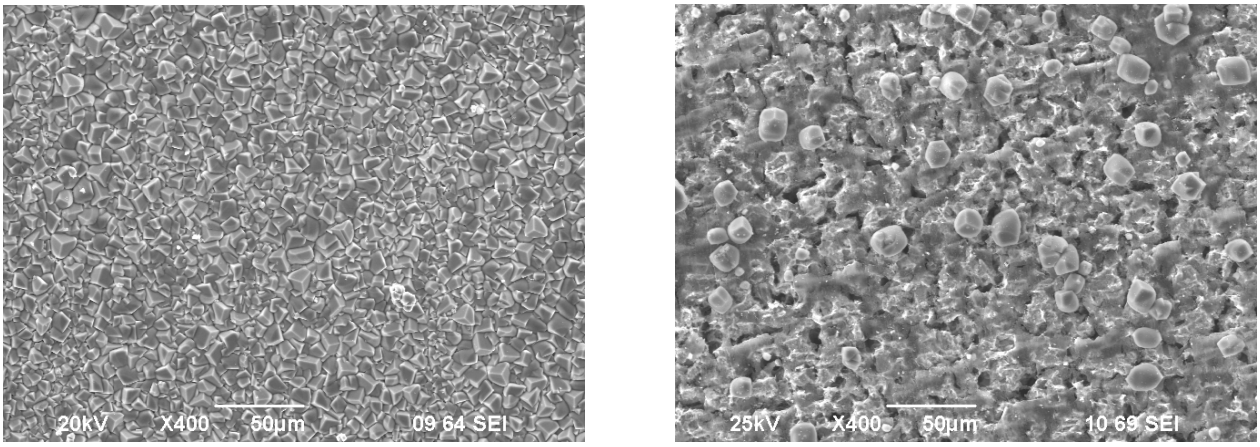

a) b)

Figure 12. $FeCO_3$ layer morphology of X-65 (pCO_2 =0.56 bar, pH 6.3, 1000rpm and T=80°C).
a) layer formed in pure CO_2 after 70 h, see Figure 11 above and
b) layer after addition of 50 ppm of undissociated acetic acid, appearance at the end of the experiment shown in Figure 11 above.

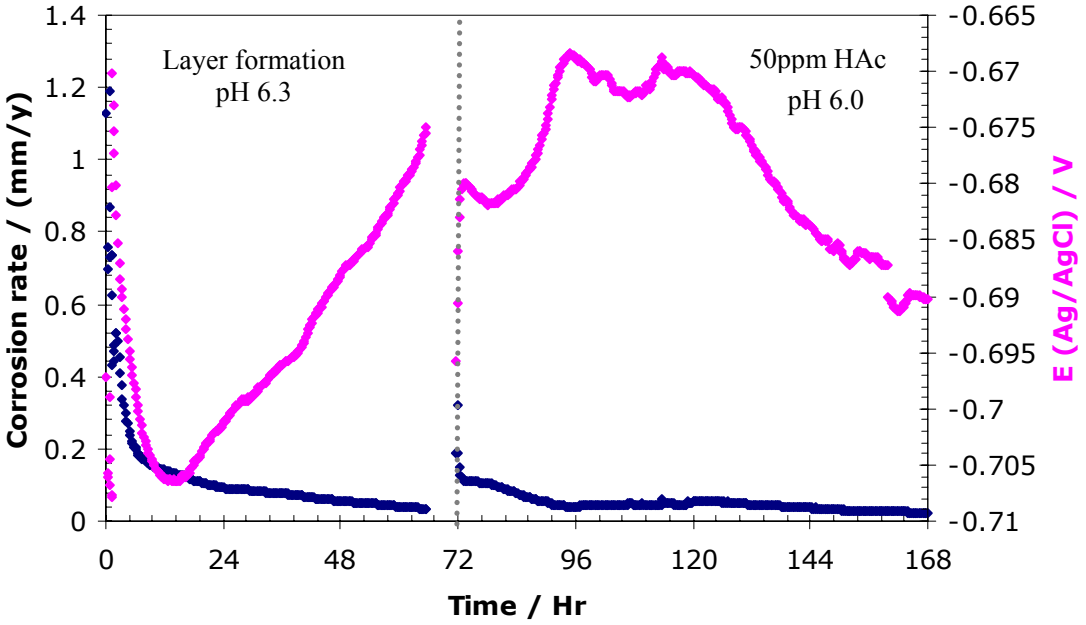

Figure 13. The effect of pH on the corrosion rate and corrosion potential of X-65 steel during 168 hours of exposure (3% NaCl, 50 ppm of undissociated acetic acid, 0.56 bar pCO_2, stagnant conditions, and T=80°C).

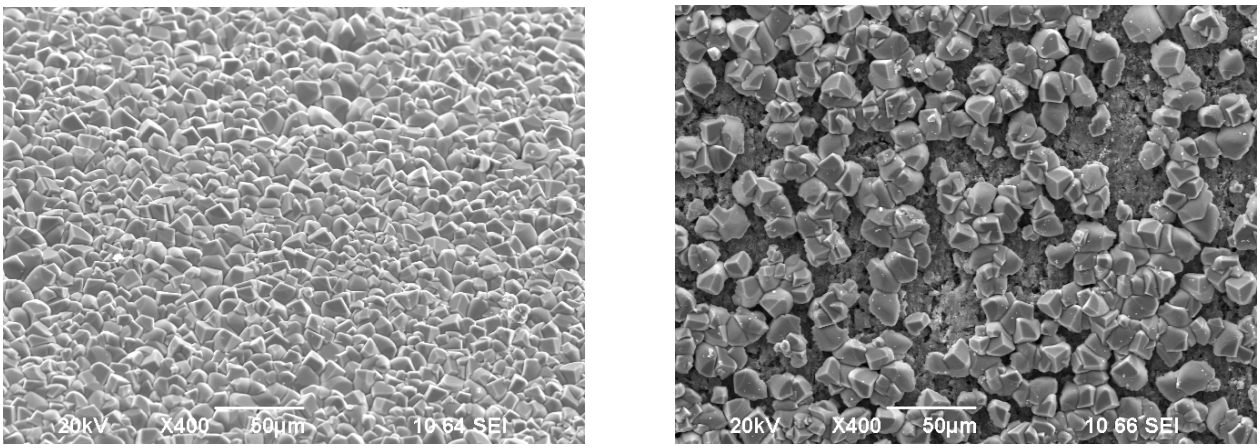

a) b)

Figure 14. $FeCO_3$ layer morphology of X-65 (pCO_2 =0.56 bar, stagnant conditions and T=80°C).
a) layer formed in pure CO_2 after 72 h, see Figure 13 above and
b) layer after addition of 50 ppm of undissociated acetic acid, appearance at the end of the experiment shown in Figure 13 above.